Size dependence of Au NP-enhanced surface plasmon resonance based on differential phase measurement

Shuwen Zeng [a,b,c], Xia Yu [c], Wing-Cheung Law [d], Yating Zhang [c], Rui Hu [a], Xuan-Quyen Dinh [b], Ho-Pui Ho [e], Ken-Tye Yong [a,*]

[a] School of Electrical and Electronic Engineering, Nanyang Technological University, Singapore 639798, Singapore
[b] CINTRA CNRS/NTU/THALES, UMI 3288, Research Techno Plaza, 50 Nanyang Drive, Border X Block, Singapore 637553, Singapore
[c] Singapore Institute of Manufacturing Technology, 71 Nanyang Drive, Singapore 638075, Singapore
[d] Institute for Lasers, Photonics and Biophotonics, State University of New York at Buffalo, Buffalo, NY 14260-3000, United States
[e] Department of Electronic Engineering, The Chinese University of Hong Kong, Hong Kong, China

ARTICLE INFO

ABSTRACT

The impact of spherical gold nanoparticles (Au NPs) with diameters of 40–80 nm for the enhancement of surface plasmon resonance (SPR) sensing signals is presented. Numerical analysis is given to simulate the perturbation of evanescent field in the presence of Au NPs. The results indicate that Au NPs with 40 nm possess the highest coupling effect when the separation of Au NP and SPR sensing film is fixed at 5 nm. For experimental demonstrations, colloidal Au NPs with different sizes but unified extinction coefficient (optical density) are immobilized onto SPR sensing films respectively through a spacer, dithiothreitol (DTT). Phase changes of the reflected SPR signals, which are associated with the plasmonic coupling between the NPs and sensing film, are monitored using a differential phase SPR sensor. Results obtained from the experiments show good agreement with the theoretical studies. This work can considerably serve as a solid guidance for future development of Au NPs-enhanced SPR sensors.

1. Introduction

Surface plasmon resonance (SPR) sensors have attracted great attention over the past decade for their powerful capability and flexibility of studying various chemical and biological interactions [1–3]. The sensing mechanism is based on the fact that very small refractive index change at the metal/dielectric interface can affect the surface plasmons excited by incident light, thereby optical characteristics (intensity, phase and polarization) of the reflected light are varied accordingly and can be monitored in real-time. In conventional SPR sensors, usually based on angle-dependent reflectance measurement, are limited for detecting low molecular weight molecules such as TNT, DNA, cytokine and hormones. So far, there are two main strategies for overcoming this drawback: (i) developing phase-sensitive SPR sensors, (ii) using nanoparticle-based detection regimes [4–8]. It is reported that by modifying the sensing film with colloidal spherical gold nanoparticles (Au NPs), gold nanocages (Au NCs) and gold nanorods (Au NRs), the sensitivity can be significantly enhanced [9–11]. Among these nanoparticles, spherical Au NPs are more favorable to the enhanced

SPR sensors because of their isotropic structures which allow the coupling to occur at every direction rather than only in the longitudinal direction for Au NRs [12]. Strong absorption of incident light followed by field enhancement on the metallic surface (Au NP and Au thin film) is a typical property of SPR excitation [2]. The principle of Au NPs-enhanced SPR is due to the strong field coupling between localized SPR (LSPR) of Au NPs and SPR of the sensing film, thus it is important to unify the LSPR of Au NPs during the size dependence study of Au-enhanced SPR. LSPR of Au NPs is represented by their extinction coefficient (or called optical density) which is determined by the absorption and scattering efficiency [13]. For Au NPs with different sizes, the absorption and scattering efficiency contribute differently to the LSPR, and therefore will lead to different field coupling effects to Au NPs-enhanced SPR sensors. Furthermore, the sensitivity of Au-enhanced SPR sensors is demonstrated to be directly related to the excited electric field strength and the perturbation (dip angle shift or phase change) of SPR curves [6,14]. However, not much effort has been given to address the size issue of Au-enhanced SPR sensors, especially for Au NPs > 40 nm. In this paper, first, we numerically investigate the correlation between evanescent field perturbations and different sizes of Au NPs (40 nm, 60 nm, 70 nm and 80 nm) with 5 nm apart from the sensor surface. Then we experimentally demonstrate the size dependence of Au NPs-enhanced SPR using differential-phase

* Corresponding author. Tel.: +65 67905444.
  E-mail address: ktyong@ntu.edu.sg (K.-T. Yong).

detection method. Using DTT as the spacer, colloidal Au NPs with diameters of 40 nm, 60 nm, 70 nm and 80 nm have been immobilized on the sensor surface for investigating their coupling effect to the enhanced SPR sensing signals.

2. Theoretical modeling

According to the conditions for surface plasmon excitation in the Kretchmann configuration [2], the wave vector of incident light projected in the x direction k_x, which is parallel to the sensing film, should be matched with the wave vector of the surface plasmon oscillations k_{sp}:

$$k_x = k_{sp} \quad \text{where} \quad k_x = k_0 n_{\text{prism}} \sin \theta_{\text{inc}} \qquad (1)$$

Here k_0 is the wave vector of the incident light in free space, $n_{\text{prism}} = 1.76552$ is the refractive index of the prism at wavelength of 785 nm, $\theta_{\text{inc}} = 52.0°$ is the incident angle. Thus, the calculated wavelength of surface plasmon λ_{sp} from Eq. (1) is 564 nm. When the absorption peak of LSPR for colloidal Au NPs is close to the wavelength of surface plasmons excited in the gold thin film λ_{sp}, strong plasmonic coupling will occur and lead to enhanced changes in the SPR signal. The absorption peaks of colloidal Au NPs used in our experiments are 525 nm, 535 nm, 541 nm and 571 nm for diameters of 40 nm, 60 nm, 70 nm and 80 nm, respectively. It is worth noting that as the Au NPs are placed close to the gold metallic film, there will be a significant red-shift (up to 100 nm) for the extinction spectrum of Au NPs, which varies with spacing distance between the particle and the sensing film [15]. Furthermore, from Mie scattering theory, in the case of Au NPs with diameter smaller than 40 nm, the extinction coefficient (absorption peak in UV–vis measurement) is dominated by the absorption of the nanoparticles. When the diameter exceeds 40 nm, the scattering component becomes more pronounced with increasing particle size [13]. As a result, Au NPs with diameter >40 nm on the sensing film would absorb less light energy and thus relatively weaker field enhancements will be excited.

To further understand how the ratio of absorption and scattering affects the plasmon coupling, we simulated the perturbation of evanescent field between the Au NPs and the sensing film using finite element analysis (COMSOL Multiphysics 3.5). Fig. 1a shows the solution space and the media in the modeling from left to right is: prism, sensing film (gold with 50 nm thickness) and water, respectively. In Fig. 1d, one can see that when there is no Au NP within close range to the sensing film, a clear evanescent field is observed when SPR occurs. Under these conditions, the electric field decays exponentially from the metallic substrate. The field intensity profiles along the direction normal to the sensing film for various Au NP-sensing film distances are presented in Fig. 1c. If we fix the size of the Au NPs, the largest enhancement of the local field is achieved when the gap is 5 nm wide. As shown in Fig. 1b, Au NPs with diameter of 40 nm has the greatest overall field enhancement in the gap (fixed at 5 nm) between the Au NPs and the sensing film, suggesting that the absorption component dominates the field enhancement. It should also be noted that the electric field amplitude obtained in the presence of Au NP has more than 2 orders of magnitude higher than that without Au NPs.

3. Experimental

3.1. Materials

DL-Dithiothreitol (BioUltra, ~1 M in H_2O), glycerin ($\geq$99%), formamide (BioReagent, $\geq$99.5%) were purchased from Sigma Aldrich. Spherical gold nanoparticles (OD = 1.0) with diameters 40 nm, 60 nm, 70 nm and 80 nm were purchased from Nanopartz Accurate.

The size variance is less than 4%. All chemicals were used as received without further purification. Ultrapure deionized (DI) water was obtained by Spectra-Teknik water purification system. Glass slides coated with 50 nm of gold film were purchased from Platypus.

3.2. SPR sensor

In order to demonstrate the aforementioned size dependence experimentally, a home-built differential phase-sensitive SPR sensor based on a modified interferometric configuration as shown in Fig. 2(a) is used. An 80-mW 785 nm laser diode is used as the excitation light source and is 45° linearly polarized for both p- and s-polarizations. In the signal beam, the light goes through a sensor head consisting of an equilateral prism made from SF11 glass (Edmund optics) and a flow chamber that allows the sample solutions to interact with the 50 nm thick sensing film (Platypus). The sensing film is attached to the prism with the aid of optical matching oil (Cargille labs). The incident angle is approximately 52.0°. In order to improve system stability, the reference arm is modified with a Michelson like configuration to avoid any temporal shift in the reflected beam due to movement of the piezoelectric transducer (PZT). The PZT is driven by a sawtooth wave oscillating at 86 Hz to generate an optical path difference and obtain complete sine waves for both p- and s-polarizations (see Fig. 2(b)). At the last beam splitter, the signal beam and reference beam interferes and is finally separated by the Wollaston prism into p- and s-polarized light. A software program (Labview 8.2) is written to collect the real-time data from the two-channel photo detector through a DAQ card (NI PCI-6115). The phase difference extraction process involves a point-wise arcsine algorithm after low-pass filtering [16].

4. Results and discussion

4.1. Performance of the SPR sensing system

Fig. 3 shows the calibration results of our home-built SPR sensing system, different weight ratios (1%, 2.5% and 5%) of glycerin and formamide solutions were introduced into the sensor head, respectively. The corresponding refractive index from pure water to 5% glycerin is 1.333–1.339 [17]. For 1% glycerin, the refractive index change from water is 0.0012 refractive index units (RIU) and a phase change of 22.16° is obtained (see Fig. 3(a)). Stability of the system was also monitored for 10 min, and the fluctuation of differential phase is approximately 0.01°. Thus, the calculated detection limit for our SPR sensor is 5.4×10^{-7} RIU. Formamide is a commonly used reagent for many biological reactions, for example, it can be used for stabilizing denatured single-strand DNA [1,18]. Calibration curves for formamide solution are very important for biosensing applications. The step-like phase change with increasing concentration of formamide in Fig. 3(b) also demonstrates the high sensitivity of our differential-phase SPR sensor.

4.2. Nanoparticle-enhanced SPR sensing measurements

According to our simulation results, a 5 nm spacer between the Au NPs and the sensing film should produce the largest evanescent field perturbation. It is known that binding of Au NPs to the surface of organic-modified substrates (metal, glass, Al_2O_3) can be achieved with covalent bonds between colloidal Au and functional groups such as —SH, —CN, —NH_2 and —COOH. Among them, thiol groups (—SH) attracted a lot of attention in the area of functionalized self-assembled monolayers (SAMs) because of their flexibility and strong binding strength in Au—S bonds [19,20]. A typical Au NP-enhanced SPR detection process is that the targeted biological or chemical analytes are first flowed onto
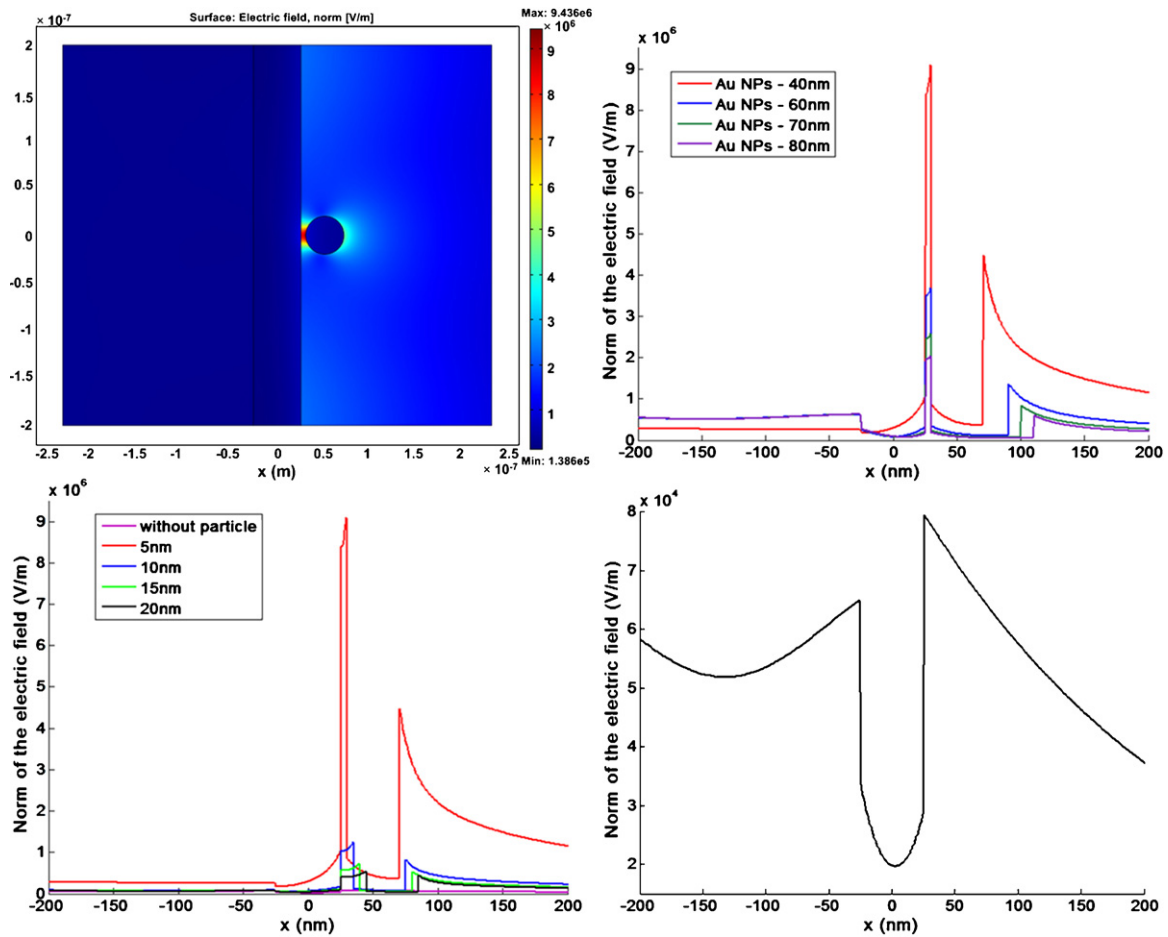
Fig. 1. FEA simulations of resonant spherical-Au NP coupling to the sensing film: (a) normal of the electric field with Au NP (diameter is 40 nm, distance from the film is 5 nm), cross-section plots for the electric field along $y = 0$, (b) Au NP with different diameters, (c) different distances between Au NP (40 nm in diameter) and the Au film, (d) without Au NP. The electric fields for Au NP with diameter in 60 nm, 70 nm and 80 nm in (b) are magnified by a factor of 10 for clarity.

the functionalized sensing film followed by Au NPs functionalized with capture-analytes. In this way, sandwich structures with targeted analytes between the Au NPs and the sensing film are formed [6]. Thiol groups are perfect candidate for functionalizing the sensing film due to their capability of binding to most of small

targeted analytes such as single strand DNA and hormones [21,22]. It is reported that when dithiothreitol (DTT) is bound to a metallic substrate, the distance introduced by the thiol-groups is estimated to be 5 nm [23–25], which matches well with our previous calculated optimal separation distance. Thus, in our configuration, DTT
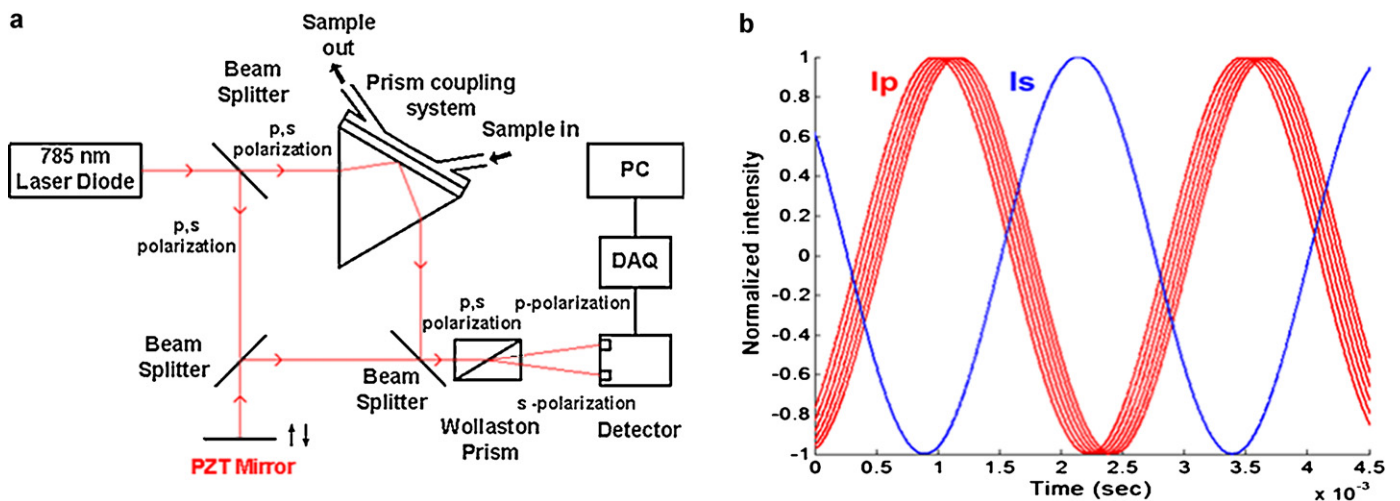

Fig. 2. (a) Schematic diagram of the differential phase-sensitive SPR sensor based on a modified interferometric configuration and (b) simulations results of I_p and I_s (n_{sample} ranging from 1.0000 to 1.0005). I_p (red curves) shifts to right with increasing n_{sample} while I_s (blue curve) remains unchanged. (For interpretation of the references to color in this figure legend, the reader is referred to the web version of the article.)
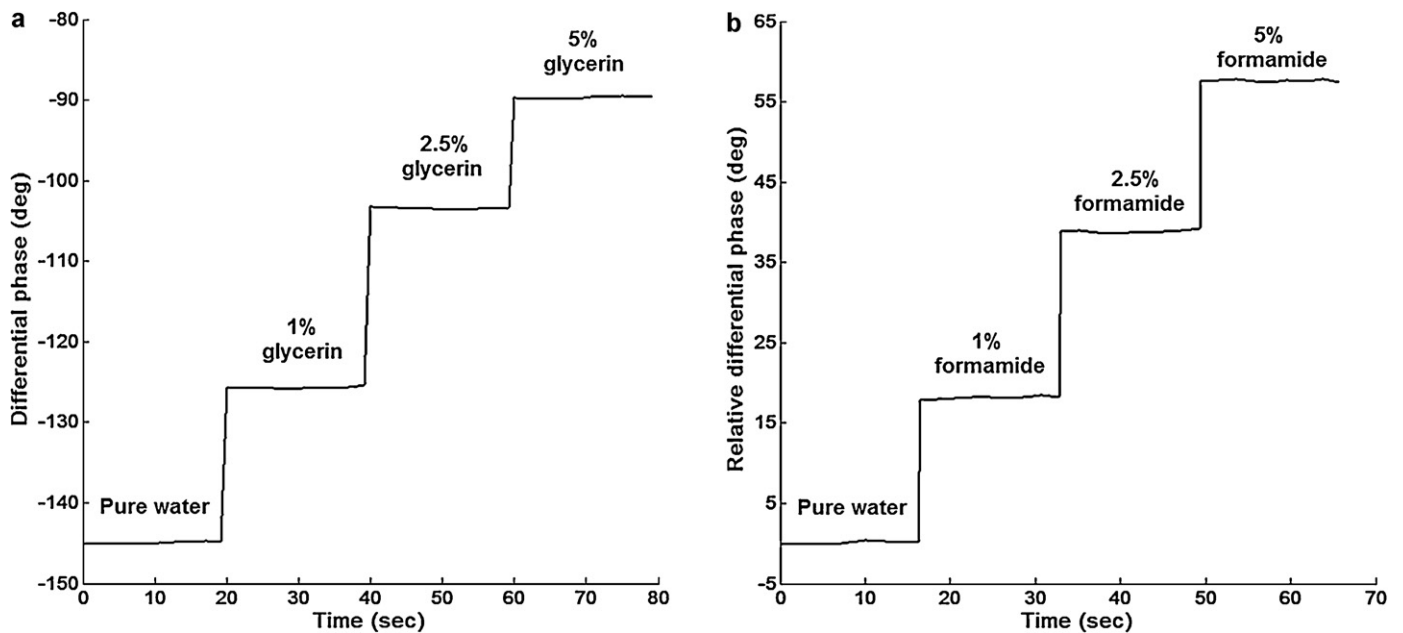
Fig. 3. Real-time differential phase measurement for various weight ratios of glycerin (a) and formamide (b) in water. In (b), the baseline was measured after flowing deionized (DI) water onto the sensor surface.

is used for surface derivatization of Au substrate where one end of the molecule is attached to the sensing film and the other end forms an Au—S bond with colloidal Au NPs (see Fig. 4). The process of sensing film functionalized with DTT was monitored by our differential phase-sensitive SPR sensor. A sharp phase change was observed upon the addition of 10 mM DTT solution onto the sensor head. The results are shown in Fig. 4(a). The system was left for a period of 20 min and then rinsed by DI water to confirm the functionalization. Longer immersion times and higher concentrations of DTT did not noticeably improve the signal change.

Fig. 5 illustrates the phase change plots after flowing colloidal Au NPs with diameters of 40 nm, 60 nm, 70 nm and 80 nm onto the sensor head. It is worth mentioning that for minimizing variations in sensing performance, the four sensing films were previously
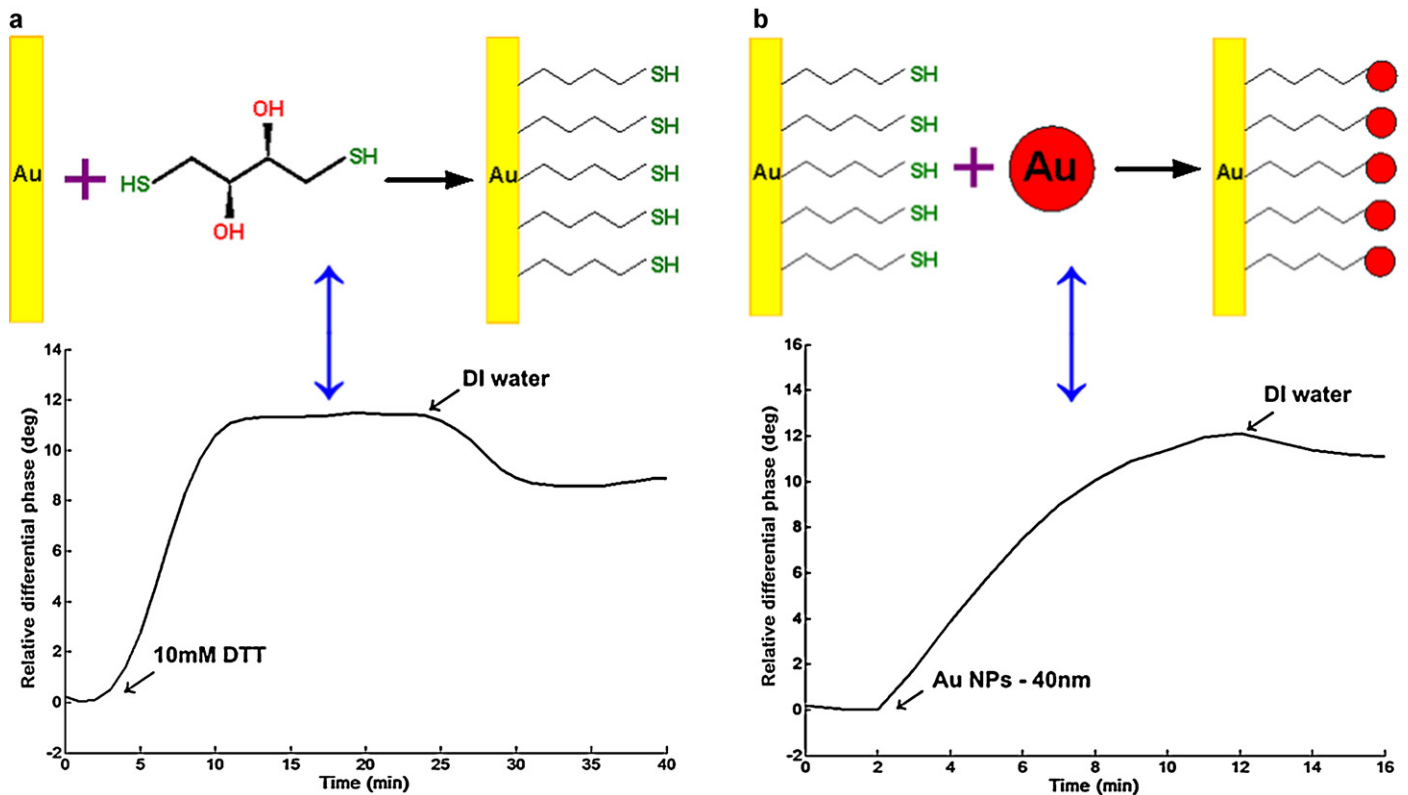

Fig. 4. Response curves obtained after flowing (a) 10 mM DTT solutions, (b) solutions of spherical Au NPs with 40 nm diameter (OD = 1.0), followed by DI water. The baseline was measured after (a) flowing deionized (DI) water onto the sensor surface, (b) the formation of DTT layer on the sensor surface.
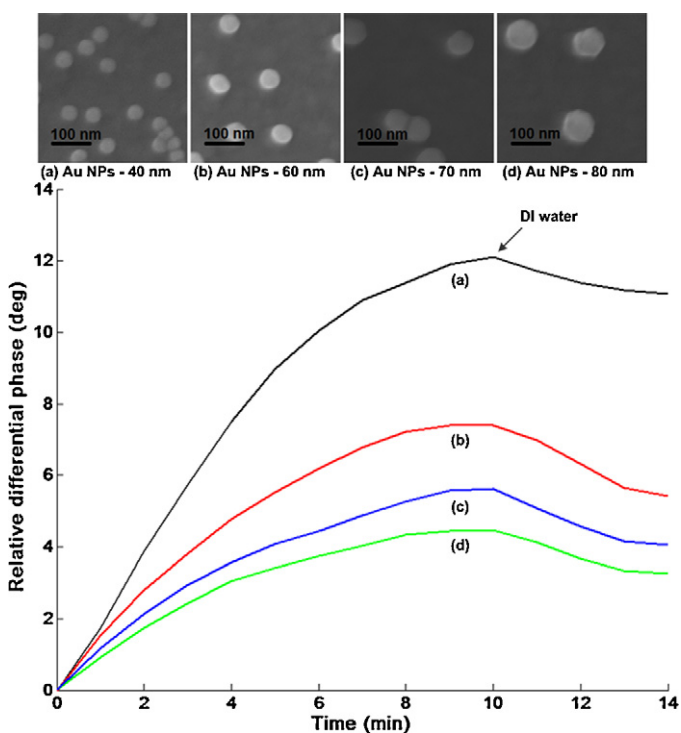
Fig. 5. Response curves obtained after flowing solutions of spherical Au NPs (OD = 1.0) with different diameters: (a) 40 nm, (b) 60 nm, (c) 70 nm, and (d) 80 nm. Inset figures are FE-SEM images of the Au NPs immobilized on gold thin films.

immersed in the solution of 10 mM of DTT for 12 h and then rinsed with water to remove any unbound thiol. The films were then stored in a nitrogen-saturated container to prevent oxidation of thiol group. The optical density (OD) value of absorption peak for all Au NPs solutions are fixed at 1.0. Baseline was established by water, response curves as shown in Fig. 5 are associated with the phase change that is obtained after binding different sizes of Au NPs onto the modified sensor surface with the layer of DTT. After 10 min reaction time, DI water was running again to confirm the binding between Au NPs and the sensing film. As one can see from Fig. 5, the SPR response curves are size dependence. The corresponding phase changes for 40 nm, 60 nm, 70 nm and 80 nm are 12.10°, 7.40°, 5.63° and 4.45°, respectively, showing good agreements with our simulation results. Field-emission scanning electron microscopy (Zeiss Ultra-Plus FE-SEM) was used to characterize the resulting sensing films and confirm that Au NPs with different diameters have been bound to the films uniformly (see inset figures in Fig. 5).

5. Conclusions

In our work, the size-dependent signal response in terms of phase change has been demonstrated in an Au NPs-enhanced SPR sensing system. The particle size used here ranges from 40 nm to 80 nm, which extinction coefficients are composed of two components: absorption and scattering. Results from differential-phase SPR measurements agree well with those obtained from theoretical modeling using finite element methods. It is revealed that the enhanced SPR sensing signals decrease with increasing particle size and Au NPs of 40 nm in diameter offers the best signal amplification factor for the SPR sensing system. This is mainly due to the fact that the influence of scattering in Au NP with diameters >40 nm becomes much stronger than the absorption. We envision that these findings reported herein will serve as a useful guidance and open a new pathway for the development of ultra-sensitive SPR sensors based on the Au NP-enhanced scheme.

References

[1] P.N. Prasad, Introduction to Biophotonics, Wiley-Interscience, New York, 2003.
[2] H. Raether, Surface Plasmons on Smooth and Rough Surfaces and on Gratings, Springer-Verlag, Berlin, 1988.
[3] J. Homola, Surface plasmon resonance sensors for detection of chemical and biological species, Chemical Reviews 108 (2) (2008) 462–493.
[4] A.V. Kabashin, S. Patskovsky, A.N. Grigorenko, Phase and amplitude sensitivities in surface plasmon resonance bio and chemical sensing, Optics Express 17 (23) (2009) 21191–21204.
[5] H.P. Ho, W. Yuan, C.L. Wong, S.Y. Wu, Y.K. Suen, S.K. Kong, C.L. Lin, Sensitivity enhancement based on application of multi-pass interferometry in phase-sensitive surface plasmon resonance biosensor, Optics Communication 275 (2) (2007) 491–496.
[6] W.C. Law, K.T. Yong, A. Baev, P.N. Prasad, Sensitivity improved surface plasmon resonance biosensor for cancer biomarker detection based on plasmonic enhancement, ACS Nano 5 (6) (2011) 4858–4864.
[7] S. Zeng, K.-T. Yong, I. Roy, X.-Q. Dinh, X. Yu, F. Luan, A review on functionalized gold nanoparticles for biosensing applications, Plasmonics 6 (3) (2011) 491–506.
[8] M. Riskin, R. Tel-Vered, O. Lioubashevski, I. Willner, Ultrasensitive surface plasmon resonance detection of trinitrotoluene by a bis-aniline-cross-linked Au nanoparticles composite, Journal of the American Chemical Society 131 (21) (2009) 7368–7378.
[9] K.M. Byun, S.J. Kim, D. Kim, Design study of highly sensitive nanowire-enhanced surface plasmon resonance biosensors using rigorous coupled wave analysis, Optics Express 13 (10) (2005) 3737–3742.
[10] S. Fang, H.J. Lee, A.W. Wark, R.M. Corn, Attomole microarray detection of MicroRNAs by nanoparticle-amplified SPR imaging measurements of surface polyadenylation reactions, Journal of the American Chemical Society 128 (43) (2006) 14044–14046.
[11] J.L. Wang, A. Munir, Z.H. Li, H.S. Zhou, Aptamer-Au NPs conjugates-enhanced SPR sensing for the ultrasensitive sandwich immunoassay, Biosensors and Bioelectronics 25 (1) (2009) 124–129.
[12] M.J. Kwon, J. Lee, A.W. Wark, H.J. Lee, Nanoparticle-enhanced surface plasmon resonance detection of proteins at Attomolar: comparing different nanoparticle shapes and sizes, Analytical Chemistry 84 (3) (2012) 1702–1707.
[13] P.K. Jain, K.S. Lee, I.H. El-Sayed, M.A. El-Sayed, Calculated absorption and scattering properties of gold nanoparticles of different size, shape, and composition: applications in biological imaging and biomedicine, Journal of Physical Chemistry B 110 (14) (2006) 7238–7248.
[14] L.A. Lyon, M.D. Musick, M.J. Natan, Colloidal Au-enhanced surface plasmon resonance immunosensing, Analytical Chemistry 70 (24) (1998) 5177–5183.
[15] J.D. Driskell, R.J. Lipert, M.D. Porter, Labeled gold nanoparticles immobilized at smooth metallic substrates: systematic investigation of surface plasmon resonance and surface-enhanced Raman scattering, Journal of Physical Chemistry B 110 (35) (2006) 17444–17451.
[16] H.P. Ho, W.C. Law, S.Y. Wu, C.L. Lin, S.K. Kong, Real-time optical biosensor based on differential phase measurement of surface plasmon resonance, Biosensors and Bioelectronics 20 (10) (2005) 2177–2180.
[17] R.C. Weast, CRC Handbook of Chemistry and Physics, 68th ed., CRC Press, Boca Raton, FL, 1987.
[18] J. Fuchs, D. Dell'Atti, A. Buhot, R. Calemczuk, M. Mascini, T. Livache, Effects of formamide on the thermal stability of DNA duplexes on biochips, Analytical Biochemistry 397 (1) (2010) 132–134.
[19] K.C. Grabar, K.J. Allison, B.E. Baker, R.M. Bright, K.R. Brown, R.G. Freeman, A.P. Fox, C.D. Keating, M.D. Musick, M.J. Natan, Two-dimensional arrays of colloidal gold particles: a flexible approach to macroscopic metal surfaces, Langmuir 12 (10) (1996) 2353–2361.
[20] R.G. Freeman, K.C. Grabar, K.J. Allison, R.M. Bright, J.A. Davis, A.P. Guthrie, M.B. Hommer, M.A. Jackson, P.C. Smith, D.G. Walter, M.J. Natan, Self-assembled metal colloid monolayers: an approach to SERS substrates, Science 267 (5204) (1995) 1629–1632.
[21] K.A. Peterlinz, R.M. Georgiadis, T.M. Herne, M.J. Tarlov, Observation of hybridization and dehybridization of thiol-tethered DNA using two-color surface plasmon resonance spectroscopy, Journal of the American Chemical Society 119 (14) (1997) 3401–3402.
[22] Y.M. Bae, B.K. Oh, W. Lee, W.H. Lee, J.W. Choi, Study on orientation of immunoglrbulin G on protein G layer, Biosensors and Bioelectronics 21 (1) (2005) 103–110.
[23] J.M. Tour, L. Jones, D.L. Pearson, J.J.S. Lamba, T.P. Burgin, G.M. Whitesides, D.L. Allara, A.N. Parikh, S.V. Atre, Self-assembled monolayers and multilayers of conjugated thiols, alpha, omega-dithiols, and thioacetyl-containing adsorbates – understanding attachments between potential molecular wires and gold surfaces, Journal of the American Chemical Society 117 (37) (1995) 9529–9534.
[24] Y.S. Shon, S. Lee, S.S. Perry, T.R. Lee, The adsorption of unsymmetrical spiroalkanedithiols onto gold affords multi-component interfaces that are

homogeneously mixed at the molecular level, Journal of the American Chemical Society 122 (7) (2000) 1278–1281.

[25] A.R. MacDairmid, M.C. Gallagher, J.T. Banks, Structure of dithiothreitol mono-layers on Au(1 1 1), Journal of Physical Chemistry B 107 (36) (2003) 9789–9792.

Biographies

Shuwen Zeng is currently a Ph.D. student of the School of Electrical and Electronic Engineering at Nanyang Technological University.

Xia Yu received the B.Eng. and Ph.D. degrees in Electrical and Electronic Engineering both from Nanyang Technological University in 2003 and 2006 respectively. She is currently a Research Scientist with Precision Measurements Group, Singapore Institute of Manufacturing Technology (SIMTech). Her research interests include surface plasmonic sensing devices, photonic crystal fibers and microstructured waveguides.

Wing-Cheung Law received his Ph.D. from the Department of Electrical Engineering of the University at Buffalo, the State University of New York (SUNY) in 2011. He is now a research assistant professor of University at Buffalo – SUNY. His research interests include surface plasmon resonance biosensors and quantum dots for bioimaging.

Yating Zhang is a Ph.D. student of the College of Optoelectronic Science and Engineering at Huazhong University of Science & Technology. She is also currently an exchange research student at Singapore Institute of Manufacturing Technology (SIMTech).

Rui Hu received his Ph.D. from the Department of Optical Engineering of Zhejiang University in 2010. He is currently a research fellow at school of Electrical and Electronic Engineering, Nanyang Technological University.

Xuan-Quyen Dinh received his Ph.D. in Physics from Ecole Normale Supérieure (ENS) de Cachan, FRANCE in 2007. He is currently the deputy-director of CNRS International-NTU-Thales Research Alliance (CINTRA), Singapore. His research interests include fiber-optic communications, micro-nano fibers for sensing applications and quantum key distribution.

Ho-Pui Ho received his B.Eng. and Ph.D. in Electrical and Electronic Engineering in the University of Nottingham in 1986 and 1990 respectively. He is now a professor at The Chinese University of Hong Kong. His research interests include optical instrumentation, photonic biosensors based on the surface plasmon resonance effect, biophotonics and materials for optical applications.

Ken-Tye Yong received his Ph.D. from Chemical and Biological Engineering in SUNY at Buffalo in 2006. Following completion of his graduate studies, he did his post-doc at the Institute for Lasers, Photonics and Biophotonics from 2006 to 2009. He is currently an Assistant Professor at the Nanyang Technological University in the School of Electrical and Electronic Engineering. His research interests include metallic nanoparticles for sensing applications and quantum dots for cancer therapy.